Ethylene polymerization over supported MAO/$(nBuCp)_2ZrCl_2$ catalysts: Influence of support properties.

R. Van Grieken*, A. Carrero, I. Suarez, B. Paredes

Department of Chemical and Environmental Technology. ESCET.

Rey Juan Carlos University, 28933, Móstoles (Madrid), Spain.

European Polymer Journal 43 (2007), 1267 – 1277

doi:10.1016/j.eurpolymj.2007.01.008

* To whom the correspondence should be addressed. Phone: 34-91-4888088. Fax: 34-91-4887068.

e-mail: rafael.vangrieken@urjc.es

ABSTRACT

The catalytic system methylaluminoxane (MAO) and bis(n-butylcyclopentadienyl)zirconium dichloride ($(nBuCp)_2ZrCl_2$) was immobilized on commercial silica, silica-alumina and aluminophosphate calcined at different temperatures. The properties of the supports were determined by using N_2 adsorption-desorption isotherms at 77 K, FT-IR spectroscopy and SEM. After aluminium and zirconium impregnation, the catalysts were analyzed by ICP-AES, FT-IR and UV-Vis spectroscopy. Ethylene polymerizations were carried out in a Schlenk tube at 70 ºC and 1.2 bar of ethylene pressure. The polyethylene obtained was characterized by GPC, DSC and SEM.

Catalysts supported on silica-alumina exhibited higher polymerization activity than those supported on silica and aluminophosphate. Besides, the activity of MAO/$(nBuCp)_2ZrCl_2$ catalytic system supported on silica-alumina and aluminophosphate decreased strongly with support calcination temperature, while remained almost constant when silica was employed as support. All these experimental features suggest a role of the support acid properties and hydroxyl group population in the generation of active polymerization species.

Keywords: Supported metallocene catalysts, silica, silica-alumina, aluminophosphate, polyethylene.

INTRODUCTION

The present stage of evolution in the polyolefin industry is mainly due to the developments in the catalysis field. The discovery of the metallocenes activated with alkylaluminoxanes allowed the synthesis of new polyolefins, with different properties from those obtained through Ziegler-Natta catalysts. Metallocene catalysts combine high activity with excellent stereoregularity in the polymerization of α-olefins. Many properties have been improved through the use of these catalytic systems, such as clarity, lower haze, less odour and improved tastelessness, higher impact resistance and better heat seal properties, just to mention a few for polyethylene as example [1, 2].

The main disadvantage of this metallocene-based polymerization technology lays in the lack of morphology control of the polymer particle and reactor fouling when these catalysts are used in homogeneous processes [3, 4]. Another important disadvantage is the requirement of large amounts of cocatalyst such methylaluminoxane (MAO). Therefore, several technical problems have been solved before metallocene catalysts started to be present in the industrial plants [5].

The immobilization of metallocene compounds on a support was already verified as a suitable solution [4]. The key point is finding a way to anchor the metallocene onto the support without losing the advantages of the homogeneous complex (high catalytic activity, stereochemical control, ability to produce copolymers with statistical comonomer distribution, etc.) while improving the morphological characteristics of the polymers and the metallocene activation in order to meet the requirements for industrial applications [5].

Find a suitable support is an important research goal in the catalyst preparation and therefore many studies have been developed to study the way to support

metallocenes [6-8]. The nature of the support as well as the technique used to anchor the metallocene, play an important role in the catalytic activity and in the final properties of the polymers, such as morphology and molecular weight distribution. On line with this, it has been reported that the support can also modify the polymer microstructure [9].

Different contributions in literature suggest that there are at least three basic methods of supporting aluminoxane-activated single-site catalysts [10]:

1) Supporting the aluminoxane and then reacting with the metal complex.

2) Supporting the metallocene and then reacting with aluminoxane.

3) Contacting the aluminoxane and metal complex in solution before supporting.

The last method maximizes the number of catalytic centres by activating the metal component in solution, instead of carrying out the process with one of the components in an immobilized state. Thus, highly active catalysts can be obtained even at low Al/Me ratios. One way for supporting this catalytic system is the "incipient wetness" method, in which the support is contacted with a minimum volume of metallocene/MAO solution just to wet the solid support. An amount proportional to the pore volume of the solid is fixed depending on the metal loading and the Al/Metal molar ratio [10, 12]. By means of the incipient wetness technique, the catalyst is placed inside the pores of the support, improving the particle morphology and reducing the volume of the solvent, besides decreasing preparation time and lowering effluents and disposal costs [13].

The chemical properties of the support play an important role for anchoring the metallocene catalytic system. Moreover, the interaction of an immobilized catalytic system with the support material is of great importance since it will strongly determine the possibility of leaching [14-16]. Several works pointed out that the immobilization is

related with the Lewis acid sites on the support surface, where the metallocene would be held in an active form [2, 17-19]. Therefore, by the choice of the right support, it is possible to obtain supported complexes for which the vicinity of Lewis acid sites will favour the partial or total transfer of the alkyl (or the halide) from the zirconium to the surface [20].

On the other hand, the morphology of the polymer particle depends strongly on the shape and structure of the employed support. It is known that during early stages of polymerization, the polymer forms a regular thin layer around the particle, which partially continues growing into the marginal areas of the micro- and mesopores of the support. As the polymerization time increases, the polymer growth from the outside to the inside continues accompanied by a slow fragmentation of the support. This fact allows the access to new active centres and the reaction proceeds until the highest possible activity is reached and the whole support is fragmented in the polymer [13].

In this work, three commercial supports such as silica, silica-alumina and aluminophosphate have been analyzed in order to consider their suitability for anchoring the $(nBuCp)_2ZrCl_2$/MAO catalytic system. The ethylene polymerization activity of heterogeneous catalysts was studied at different support calcination temperatures to module the reactivity of the support surface.

EXPERIMENTAL

Preparation of supported catalytic systems

Silica, silica-alumina (Si/Al = 4.8; Al = 5.48 wt %) and aluminophosphate (P/Al= 1; Al = 23 wt%) materials supplied by Grace-Davison were employed to support the MAO/$(nBuCp)_2ZrCl_2$ catalytic system. Heterogeneous catalysts were prepared by

impregnating commercial supports (uncalcined or calcined at different temperatures) with a mixture containing a solution of methylaluminoxane (MAO 30 wt% in toluene, Witco) and a solution of bis(butylcyclopentadienyl)zirconium dichloride ($(nBuCp)_2ZrCl_2$, Crompton) in dry toluene under inert nitrogen atmosphere using the Schlenk technique and glove box. The amounts of MAO and metallocene were calculated in order to get supported catalysts with an Al_{MAO}/Zr molar ratio of 170).

The impregnations were performed at room temperature, in a stirred vessel during 3 hours with a volume of impregnating solution equal to three times the pore volume of the support. Then, the solids were dried under nitrogen flow and stored in glove-box.

Polymerization reactions

Ethylene polymerizations were performed in a Schlenk tube kept at 70 ºC in an oil bath and 1.2 bar of ethylene pressure. Solid catalyst was suspended in 20 mL of heptane and transferred to the Schlenk where tri-isobutylaluminium (TIBA, 30 wt% in heptane, Witco) was added as scavenger to get an Al(TIBA)/Zr molar ratio of 800. After 30 minutes, polymerization reaction was stopped by depressurization and quenched by addition of acidified (HCl) methanol. The polyethylene obtained was separated by filtration and dried under atmospheric pressure at 70 ºC. All reactions were done twice and the activity values reported are the average between both experiments.

Characterization of supports, catalysts and polyethylenes

N_2 adsorption-desorption isotherms at 77 K were obtained on a Micromeritics TRISTAR 2050 sorptometer. Prior to the adsorption, the supports were outgassed under vacuum at 200 ºC for 2 h. Surface areas were calculated according to the BET method

whereas pore size was obtained from the maximum of the BJH pore size distribution curve.

FT-IR spectra were recorded on a ATI Mattson Infinity Series spectrometer. The samples were placed in a catalytic chamber HVC-DPR (Harrick Scientific Company) where they were calcined under vacuum ($<10^{-4}$ mbar) at different temperatures. UV-Vis spectroscopic studies of MAO/$(nBuCp)_2ZrCl_2$ supported catalysts were performed in a Varian Cary 500 spectrophotometer. Catalyst samples were sealed, in the glove box, into 1 centimetre quartz cells with Teflon stoppers. The UV-Vis spectra were scanned (450 nm/min) using an integrating sphere diffuse reflectance accessory to enable the measurement in reflectance mode.

Aluminium and zirconium contents of the supported catalysts were determined by ICP-AES on a Varian Vista AX Axial CCD Simultaneous ICP-AES spectrophotometer.

In order to analyze the morphology and the particle size of the supports and the obtained polyethylenes, scanning electron microscopy (SEM) was used with a Phillips XL30 ESEM (Environmental Scanning Electron Microscope) equipped with a tungsten filament and an accelerating voltage of 15 kV. Master Sizer 2000 Malvern Instruments was used to determine the particle size distribution.

Polymers mean molecular weight and molecular weight distributions were determined by size-exclusion chromatography at 145°C on a Waters 150C Plus instrument, using 1,2,4-trichlorobenzene as mobile phase. The column set consisted of one PL-Gel 10μm Mixed B (300 x 7.5 mm) and another Polymer PL-Gel 10 μm 10E6A (300 x 7.5 mm). The columns were calibrated with 11 polystyrene standards

(narrow molar mass distribution in the range: 2960-2700000) and with one high polydispersity polyethylene standard (NIST, Mw = 53070).

Polymer melting points (T_m) and crystallinities were determined using a METTLER TOLEDO DSC822 differential scanning calorimeter, with a heating rate of 10 ºCmin^{-1} from 23 to 160 ºC. The heating cycle was performed twice, but only the results of the second scan are reported to avoid the influence of the mechanical and thermal history of the samples.

RESULTS AND DISCUSSION

Supports characterization

The main physical properties of the commercial materials used as supports for the catalytic system $(nBuCp)_2ZrCl_2$/MAO are summarized in Table 1. It is only remarkable the pore volume and size decrease experimented by silica-alumina calcined at 600 ºC, while the textural properties of the other samples remained almost unaltered.

Because the polymer particle replicates the morphology of the supported catalyst, it is important to have a carrier with the desired morphology and particle size. Figure 1 shows the scanning electron micrographs of the supports, where a well-defined spherical morphology is observed for the commercial silica with a narrow particle size distribution centred around 56 μm whereas slightly higher mean particle size (90 μm) and broader distribution is observed for SiO_2-Al_2O_3. However, $AlPO_4$ support presents an irregular morphology and very broad particle size distribution.

The thermal treatment of the support has a drastic influence on its surface chemistry and, therefore, on the type of the species formed upon contact with the metallocene system [5, 21]. The presence of surface hydroxyl groups have been studied

by infrared spectroscopy because the $\nu_{(OH)}$ absorption is strong, mainly in the range 3800-3200 cm^{-1}.

Figure 2 presents FT-IR spectra of silica, silica-alumina and aluminophosphate supports calcined at different temperatures. The interpretation of the spectra of uncalcined supports (not shown) is difficult because of the breadth of the bands due to the physisorbed water. The spectra of silica calcined between 200- 600 ºC, show a sharp band at 3736 cm^{-1} assigned to isolated silanol groups (scheme 1; I) and a shoulder at 3665 cm^{-1} due to the contribution of the so-called vicinal OH groups which undergo H-bond interactions with neighbouring silanol groups (scheme 1; II) and geminal silanols (scheme 1; III) [22-25]. In the same way, the spectra of calcined silica-alumina have a band at 3650 cm^{-1} and also a sharp band corresponding to isolated silanol groups centred at 3736 cm^{-1}. The 3650 cm^{-1} band is quite broad since OH stretching vibration in the AlOH and SiOH groups lie close together so that they overlap strongly and give the appearance of a single band [26, 27].

The spectra of calcined aluminophosphate present a narrow band at 3674 cm^{-1} assigned to the nonbonded surface P-OH groups and, a broad band around 3610 cm^{-1} which corresponds to surface hydroxyl groups perturbed by a hydrogen bridge bond from another surface hydroxyl group [28]. In general, increasing support calcination temperature, the surface OH density decreases and the bands assigned to isolated Si-OH and P-OH groups at 3736 and 3674 cm^{-1} respectively, increases in intensity. On the contrary, the broad bands placed at 3650-3660 cm^{-1} in silica and silica-alumina and at 3610 cm^{-1} in aluminophosphate decrease and finally disappear. It is noticeable how the surface of aluminophosphate calcined at 600 ºC is almost dehydroxylated since OH bands have almost disappeared.

The reaction between support surface and metallocenes takes place by elimination of one or more of the original organometallic ligands (such as halide or alkyl) in a 1:1 ratio with hydrogen atoms from hydroxyl groups (-OH) in the support, forming complexes suitable to act as active centres when a cocatalyst is added [1]. In some cases, these hydroxyl groups can induce a deleterious effect on the catalyst attributed to the decomposition of the complex, which should be avoidable by spacing such catalytic species on the support surface, through a spacer group, improving the monomer access to the active centres of polymerization [29]. In the case of MAO-mediated systems, the support is previously modified with MAO prior to metallocene immobilization [30]. In this way MAO acts as a spacer because it can be fixed through the support hydroxyl groups [31].

As an alternative, the supporting technique employed in this work consists in the addition onto the support material of a mixture with the metallocene $(nBuCp)_2ZrCl_2$ and methylaluminoxane in toluene. In order to check how the anchorage affects to the support, figure 3 shows the spectra obtained by FT-IR of silica support calcined at 200 and 600 ºC before and after the immobilization of the MAO/$(nBuCp)_2ZrCl_2$ catalyst by incipient wetness impregnation. In both spectra and independently of silica calcination temperature, the 3736 cm^{-1} band associated with isolated silanol groups disappears after the impregnation. The presence of a broad band at 3615 cm^{-1} can be attributed to silica terminal OH-groups, bound by hydrogen bonds with oxygen atoms or methyl groups of adsorbed MAO oligomeric molecules [32]. According to Panchenko et al. [17], when MAO with high content of trimethylaluminium (TMA) is used for silica treatment, most of silica terminal OH-groups interacts particularly with TMA. The absence of 3736 cm^{-1} band in the spectra of silica supported catalysts suggests the reaction of the TMA contained in the MAO/$(nBuCp)_2ZrCl_2$ solution with the terminal OH groups. Besides,

in the spectra of silica supported catalysts (Figure 3 b,d,), the new bands at 3133 and 3033 cm^{-1} correspond to the stretching vibrations of the methyl groups in the methylaluminoxane and in the $–Al–CH_3$ fragments of surface alkylaluminium compounds formed in the reaction between silica isolated silanol groups and TMA contained in MAO (scheme 2) [17].The reaction of silica-alumina and aluminophosphate supports with MAO/$(nBuCp)_2ZrCl_2$ catalytic system also produced the elimination of isolated Si-OH and P-OH groups respectively, indicating the hydrolysis of residual TMA contained in MAO.

Catalyst characterization

Metallocenes complexes need to be activated before using them as catalysts in olefin polymerization. Activation reaction steps can be observed in the UV-Vis spectrum in the following ways: a ligand to metal charge transfer (LMCT) absorption band shift to higher energies corresponding to methylation and a LMCT band shift to lower energies due to cationisation [33]. MAO reacts with $(nBuCp)_2ZrCl_2$ by abstracting the chloride ions and replacing them with one methyl group and a positive charge. This also decreases the electron density at the zirconium atom, which leads to a concomitant decrease in the energy of the LMCT because electron density is more easily transferred from the electron-rich n-butylcyclopentadienyl ligands to the electron-poor metal.

Figure 4 presents the UV-Vis spectra of MAO/$(nBuCp)_2ZrCl_2$ catalysts supported on silica, silica-alumina and aluminophosphate calcined at different temperatures. Since zirconocene was allowed to react with MAO prior to addition onto the supports, the intense band observed at 263 nm with a shoulder at 270 nm, may be related with the interactions between the supports and methylaluminoxane molecules

non reacted with $(nBuCp)_2ZrCl_2$ metallocene catalyst [34]. In general, the broad band placed around 350 nm suggests the presence of the catalyst precursor mono- and/or dimethylated together with cationic zirconium species like $[(nBuCp)_2ZrCH_3]^+[MAOCl]^-$ [33, 34]. For MAO/$(nBuCp)_2ZrCl_2$/silica and MAO/$(nBuCp)_2ZrCl_2$/silica-alumina heterogeneous catalysts, as support calcination temperature increases the LMCT band becomes narrower and slightly shifted to higher wavelengths (360 nm). On the other side, the UV-Vis spectra of catalysts supported on aluminophosphate calcined at higher temperatures (400 - 600 ºC) present a strong decrease in the intensity of the bands related with anchored MAO and metallocene active species.

Table 2 shows the aluminium loading and the Al/Zr molar ratio on the support after the impregnation procedure showing similar values independent of the support or the calcination temperature used.

Polymerization activity and polyethylene properties

The ethylene polymerization results over heterogeneous MAO/$(nBuCp)_2ZrCl_2$ catalytic system are shown in figure 5. At calcination temperatures up to 200 ºC, catalysts supported on silica-alumina and aluminophosphate are more active than those supported on silica. This fact may be related with the presence of Al^{3+} ions generating Lewis acid sites on silica-alumina and aluminophosphate supports. The presence of Lewis acid sites interacting with MAO may favour the stability of the zirconium cations (Scheme 3) and hence, the active species for polymerization [20]. This fact are in concordance with the findings of Damiani et al., [35] who observed an increase in activity when an adequate amount of $AlCl_3$ (Lewis acid) was added to the $EtInd_2ZrCl_2$/MAO system in ethylene polymerization. Besides, it has been reported that the formation and stabilization of zirconium cations (Zr^+) may be easier when support materials present surface acidic properties [5, 36]. In this sense, the best catalytic

performance of silica-alumina could be attributed to the higher acidity of Al-OH groups compared with P-OH and Si-OH [37-38].

In general, the polymerization activity of catalysts supported on silica is almost independent of carrier calcination temperature, while MAO/$(nBuCp)_2ZrCl_2$ catalysts anchored on silica-alumina and aluminophosphate showed a decrease in ethylene polymerization activity by increasing the calcination temperature of both supports. This trend must be related with the decrease in the support hydroxyl group population by increasing the calcination temperature. The interactions of MAO, TMA, and TMA-depleted MAO with a silica surface and the performance of the finished catalyst system have been studied by several groups using various analytical, spectroscopic, and theoretical techniques [11]. It is known that OH groups can react with residual TMA (scheme 2) and with Al-CH_3 groups of MAO that remain after the exchange with chlorine from the metallocene complex, allowing the fixation of the catalyst [15, 29]. The in situ hydrolysis of TMA induces the formation of additional methylaluminoxane, which may be responsible of the higher polymerization activity observed in figure 5 for uncalcined supports [22]. These findings are in agreement with the highly active heterogeneous metallocene catalysts prepared when the support is pretreated at relatively low temperatures, i.e., when a fairly high number of OH groups is present [39-43]. This result reinforces the idea that the reaction between silanol groups and an organoaluminium compound, either TMA or MAO, might be a very important step in the formation of the catalytic species.

In line with this explanation, the strong dehydroxylation of aluminophosphate support calcined at 600 ºC (see figure 2) may be responsible of the low activity achieved.

Table 2 resumes the properties of obtained polymers. All catalysts produce polymers with melting temperatures around 133-134 ºC, indicating the formation of

linear high-density polyethylene [44]. The crystallinity values (between 57-67 %) and, the molar masses for the polyethylenes obtained with MAO/$(nBuCp)_2ZrCl_2$ supported catalysts were relatively independent for silica, silica-alumina and aluminophosphate supports. The polydispersity index (Mw/Mn) remained comprised between 3.10 and 3.96, relatively higher than those values expected for homogeneous single-site catalysts [3], suggesting some heterogeneity in the nature of the active sites [45].

In order to check the polymer morphology, SEM micrographs of PE samples were taken and showed in figure 6. Spherical polyethylene particles were obtained with $(nBuCp)_2ZrCl_2$/MAO supported catalysts, with acceptable sizes to the adequate processing. The spherical morphology of the polymer confirmed that no homogeneous reaction took place and therefore, the catalytic system is well anchored on the commercial supports. The mean particle size for the polyethylene obtained with catalyst supported on SiO_2 is around 230 μm, 270 μm for the SiO_2-Al_2O_3 and finally 520 μm for $AlPO_4$ values directly related with the different support particle size (figure 1).

CONCLUSIONS

In this work several commercial supports SiO_2, SiO_2-Al_2O_3 and $AlPO_4$ have been calcined at different temperatures and tested as support of the MAO/$(nBuCp)_2ZrCl_2$ catalytic system.

Catalysts supported on SiO_2-Al_2O_3 and $AlPO_4$ exhibited higher polymerization activity than silica especially at lower calcination temperatures. In this sense, P-OH and Al-OH hydroxyl groups are more acidic than Si-OH and it seems that the formation and the stabilization of zirconium cations (Zr^+) may be easier when support materials present acid sites. Besides, the support hydroxyl group population has a strong influence

on polymerization activity since OH groups react with residual TMA. The in situ hydrolysis of TMA induces the formation of additional MAO, which may be responsible of the increase in activity. For these reason MAO/$(nBuCp)_2ZrCl_2$ anchored to uncalcined supports offer the best polymerization activity results.

Polymer characterization indicated the formation of high-density polyethylene. The crystallinity and molar masses values for the polyethylenes obtained with MAO/$(nBuCp)_2ZrCl_2$ supported catalysts were relatively independent for silica, silica-alumina and aluminophosphate supports. The round-shape morphology and the results of the particle size distribution of the polymers confirm that no homogeneous reaction took place and therefore, the catalytic system is well anchored, and the replica phenomena succeed during the polymerization reaction.

ACKNOWLEDGEMENTS

We gratefully acknowledge financial support from REPSOL-YPF and to Dr. Luis Mendez for particle size distribution measurements and fruitful discussions.

REFERENCES

1. Bianchini D, Stedile FC, dos Santos JHZ. Effect of MAO silica surface loading on $(nBuCp)_2ZrCl_2$ anchoring n catalyst activity and on polymer properties. Appl Catal A-Gen 2004; 261(1): 57-67.

2. Dos Santos JHZ, Larentis A, da Rosa MB, Krug C, Baumvol IJR, Dupont J, Stedile FC, Forte MDC.Optimization of silica-supported bis(butylcyclopentadienyl)zirconium dichloride catalyst for ethylene polymerization. Macromol Chem Phys 1999; 200(4): 751-757.

3. Fink G, Mülhaupt R, Brintzinger HH. Ziegler Catalyst: Recent Innovations and Technological Improvements. Berlin: Springer-Verlag, 1995.

4. Marques M de FV, De Alcantara M. Alumina as support for metallocene catalyst in ethylene polymerization. J Polym Sci Pol Chem 2003; 42(1): 9-21.

5. Ribeiro MR, Deffieux A, Portela MF. Supported Metallocene Complexes for Ethylene and Propylene Polymerizations: Preparation and Activity. Ind Eng Chem Res 1997; 36(4): 1224-1237.

6. Ciardelli F, Altomare A, Michelotti M. From homogeneous to supported metallocene catalysts. Catal Today 1998; 41(1-3): 149-157.

7. Dos Santos JHZ, Ban HT, Teranishi T, Uozumi T, Sano T, Soga K. Supported metallocenes using inorganic-organic hybrid xerogels. J Mol Catal A-Chem 2000; 158(2): 541-557.

8. Kaminsky W. Zirconocene catalysts for olefin polymerization. Catal Today 1994; 20(2): 257-72.

9. Ciardelli F, Altomare A, Bronco S. Supported metallocenes: monosite and multisite catalysts for olefin polymerization. Stud Surf Sci Catal. 2000; 130A: 187-195.

10. Hlatky GG. Heterogeneous single-site catalysts for olefin polymerization. Chem Rev 2000; 100(4): 1347-1376.

11. Severn JR, Chadwick JC, Duchateau R, Friederichs N. "Bound but Not Gagged"-Immobilizing Single-Site α-Olefin Polymerization Catalysts. Chem Rev 2005; 105: 4073-4147.

12.Vaughn GA, Speca AN, Brant P, Canich, JAM. Olefin polymerization catalyst systems, their production and use. U.S. Patent 5,863,853, 1999.

13.Brinen JL, Speca AN, Tormaschy K, Russell KA. Making supported polymerization catalyst systems, and catalyst systems therefrom. U.S.Patent 5,665,665, 1997.

14. Steinmetz B, Tesche B, Przybyla C, Zechlin J, Fink G. Polypropylene growth on silica-supported metallocene catalysts. A microscopic study to explain kinetic behaviour especially in early polymerization stages. Acta Polymerica 1997; 48(9): 392-399.

15. Fink G, Steinmetz B, Zechlin J, Przybyla C, Tesche B. Propene Polymerization with Silica - Supported Metallocene / MAO Catalysts. Chem Rev 2000; 100(4): 1377-1390.

16. Duchateau R. Incompletely Condensed Silsesquioxanes: Versatile Tools in Developing Silica-Supported Olefin Polymerization Catalysts. Chem Rev 2002; 102(10): 3525-3542.

17. Pavia L, Lampman GM, Kriz GS. Introduction to Organic Laboratory Technics; W. B. Saunders Co.: Philadelphia, PA, 1976.

18. Panchenko VN, Semikolenova NV, Danilova IG, Paukshtis EA, Zakharov VA. IRS study of ethylene polymerization catalyst SiO_2/methylaluminoxane/zirconocene. J Mol Catal A- Chem 1999; 142(1): 27-37.

19. Yunusov SM, Moroz BL, Ivanova AS, Likholobov VA, Shur VB. Anionic ruthenium cluster $K_2[Ru_4(CO)_{13}]$ as precursor of catalytically active ruthenium particles and potassium promoter. New efficient ammonia synthesis catalysts based on supported $K_2[Ru_4(CO)_{13}]$. J Mol Catal A-Chem 1998; 132(2-3): 263-265.

20. Jezequel M, Dufaud V, Ruiz-Garcia MJ, Carrillo-Hermosilla F, Neugebauer U, Niccolai GP, Lefebvre F, Bayard F, Corker J, Fiddy S, Evans J, Broyer JP, Malinge J, Basset JM. Supported metallocene catalysts by surface organometallic chemistry. Synthesis, characterization, and reactivity in ethylene polymerization of oxide-supported mono- and biscyclopentadienyl zirconium alkyl complexes: establishment of structure/reactivity relationships. J Am Chem Soc 2001; 123(15): 3520-3540.

21. Van Grieken R, Calleja G, Serrano D, Martos C, Melgares A, Suarez I. The role of the hydroxyl groups on the silica surface when supporting metallocene/MAO catalysts. Polym React Eng 2003; 11(1): 17-32.

22. Dos Santos JHZ, Krug C, Barbosa Da Rosa M, Stedile FC, Dupont J, Forte MDC. The effect of silica dehydroxylation temperature on the activity of SiO_2-supported zirconocene catalysts. J Mol Catal A-Chem 1999; 139(2-3): 199-207.

23. Iler RK. The chemistry of silica: solubility, polymerization, colloid and surface properties and biochemistry. New York, Wiley, 1979 p.892.

24. Burneau A, Barres O, Gallas JP, Lavalley JC. Comparative study of the surface hydroxyl groups of fumed and precipitated silicas. 2. Characterization by infrared spectroscopy of the interactions with water. Langmuir 1990; 6(8): 1364-1372.

25. Morrow BA, Hardin, AH. Raman spectra of some hydrogen sequestering agents chemisorbed on silica. J Phys Chem A 1979; 83(24): 3135-3141.

26. Basila MR. An infrared study of a silica-alumina surface. J Phys Chem 1962; 66: 2228-2238.

27. Peri JB, Hannan RB. Surface hydroxyl groups on γ-alumina. J Phys Chem 1960; 64: 1526-1530.

28. Rebenstorf B, Lindblad T, Andersson S, Lars T. Amorphous aluminum phosphate as catalyst support. 2. Characterization of amorphous aluminum phosphates. J Catal 1991; 28(2): 293-302.

29. Dos Santos JHZ, Greco PP, Stedile FC, Dupont J. Organosilicon-modified silicas as support for zirconocene catalyst. J Mol Catal A-Chem 2000; 154(1-2): 103-113.

30. Tait PJ, Ediati R. Metalorganic Catalysts for Synthesis and Polymerization. Springer, Heidelberg, 1999, p. 307.

31. Juan A, Damiani D, Pistonesi C. Study of zirconocene and MAO interaction with SiO_2 surfaces. Appl Surf Sci 2000; 161(3-4): 417-425.

32. Bianchini D, dos Santos ZJH, Uozumi T, Sano T. Characterization of MAO - modified silicas. J Mol Catal A: Chem 2002; 185(1-2): 223-235.

33. Mäkelä-Vaarne NI, Kallio Ka, Reichert KH, Leskelä MA. Effect of light exposure on UV-vis spectrum of $[(nBuCp)_2ZrCl_2]$ based catalyst. Macromol Chem Phys 2003; 204(8): 1085-1089.

34. Coevoet D, Cramail H, Deffieux A. UV/visible spectroscopic study of the rac-Et(Ind)$_2$ZrCl$_2$/MAO olefin polymerization catalytic system. Part 1. Investigation in toluene. Macromol Chem Phys 1998; 199(7): 1451-1457.

35. Belelli PG, Ferreira ML, Damiani DE. Addition of lewis bases and acids. Effect on α-olefins polymerization with soluble metallocenes, 1 ethylene. Macromol Chem Phys 2000; 201(13): 1458-1465.

36. Costa Vayá VI, Belelli PG, Dos Santos JHZ, Ferreira ML, Damián DE. Influence of acidic support in metallocene catalysts for ethylene polymerization. J Catal 2001; 204: 1-10.

37. McDaniel MP. Supported chromium catalysts for ethylene polymerization. Adv Catal 1985; 33: 47-98.

38. Zhao XS, Lu GQ. Aluminophosphate - based mesoporous molecular sieves: synthesis and characterization of TAPOs. Micropor Mesopor Mat 2001; 44-45: 185-194.

39. Low MJD, Severdia AG, Chan J. Reactive silica. XV. Some properties of solids prepared by the reaction of trimethylaluminum with silica. J Catal 1981; 69(2): 384-391.

40. Chang, M. Olefin polymerization catalysts from tryalkylaluminum mixture silica gel and a metallocene. U.S. Patent 5,006,500,1991.

41. Chang, M. Preparing metallocene-aluminoxane/silica gel polymerization catalysts. U.S. Patent 5,086,025, 1992.

42. Lee, D.-h.; Shin, S.-y., Lee, D.-h. Ethylene polymerization with metallocene and trimethylaluminum-treated silica. Macromol Symp 1995; 97: 195-203 .

43. Tait PJ, Ediati R, Proceedings of MetCon'97, June 4–5, 1997, Houston, USA.

44. Billmeyer, FW, "Textbook of Polymer Science" .Wiley, New York, 1984 pp. 332, 366.

45. Bianchini D, Bichinho KM, dos Santos JHZ. Polyethylenes produced with zirconocene immobilized on MAO-modified silicas. Polymer 2002; 43(10): 2937-2943.

FIGURE CAPTIONS

Figure 1. Scanning electron micrographs and particle size distributions of supports: (a) SiO_2 (b) SiO_2-Al_2O_3 and (c) $AlPO_4$.

Figure 2. FT-IR spectra of supports calcined at different temperatures: (a) 200 ºC, (b) 400 ºC, (c) 600 ºC.

Figure 3. FT-IR spectra of (a) SiO_2 support calcined at 200ºC, (b) CAT-SiO_2-200, (c) SiO_2 support calcined at 600ºC, (d) CAT-SiO2-600.

Figure 4. UV-Vis spectra of MAO/$(nBuCp)_2ZrCl_2$ catalyst supported on (I) SiO_2 , (II) SiO_2-Al_2O_3 , (III) $AlPO_4$ calcined at different temperatures : (a) uncalcined (b) 200 ºC (c) 400 ºC and (d) 600 ºC.

Figure 5. Average ethylene polymerization activity versus the support calcination temperature. Polymerization conditions: Zr: 0.0015 mmol; 200 ml heptane; ethylene pressure: 1.2 bar; temperature: 70 ºC; time: 30 minutes; TIBA was used as scavenger $Al_{(TIBA)}/Zr = 800$.

Figure 6. Scanning electron micrographs and particle size distributions of polyethylene obtained with the MAO/$(nBuCp)_2ZrCl_2$ catalyst supported on (a) SiO_2 (b) SiO_2-Al_2O_3 and (c) $AlPO_4$.

Table 1. Physical properties of the employed supports.

Support	Calcination temperature (ºC)	Average pore diameter (nm)	BET surface area (m^2/g)	Pore volume (cm^3/g)
SiO_2	--	27.7	241	1.67
	200	29.5	276	1.81
	400	28.5	285	1.55
	600	28.7	284	1.68
SiO_2-Al_2O_3	--	19.6	363	1.25
	200	18.2	370	1.29
	400	18.4	376	1.30
	600	14.8	365	1.17
$AlPO_4$	--	19.4	204	1.01
	200	19.4	208	1.05
	400	18.0	220	1.07
	600	18.9	221	1.04

Table 2. Al/Zr molar ratio of supported catalysts and properties of the polyethylenes obtained with them.

Catalytic system	Al (wt%)[a]	Al_{MAO}/Zr[a]	Polyethylene properties		
			Crystallinity (%)	$\overline{M}_w$	$\overline{M}_w / \overline{M}_n$
CAT-SiO_2	23.78	145.6	67	207783	3.74
CAT-SiO_2-200	21.03	165.5	62	196419	3.89
CAT-SiO_2-400	19.76	152.1	63	174092	3.27
CAT-SiO_2-600	13.75	177.7	63	179270	3.79
CAT-SiO_2-Al_2O_3	17.48	134.2	66	159601	3.77
CAT- SiO_2-Al_2O_3 -200	15.93	155.7	67	163462	3.64
CAT- SiO_2-Al_2O_3 -400	18.75	133.4	64	173985	3.74
CAT- SiO_2-Al_2O_3 -600	18.03	136.9	61	203317	3.78
CAT-$AlPO_4$	30.23	169.0	64	158885	3.10
CAT-$AlPO_4$-200	37.80	159.9	67	206230	3.96
CAT-$AlPO_4$-400	36.74	173.4	59	214840	3.70
CAT-$AlPO_4$-600	36.52	167.1	57	191392	3.56

[a] Catalysts aluminium content and Al from MAO to Zr molar ratio calculated from ICP-AES analysis.

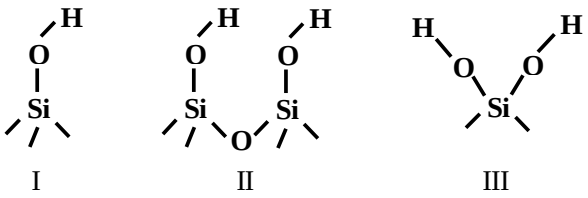

I II III

Scheme 1

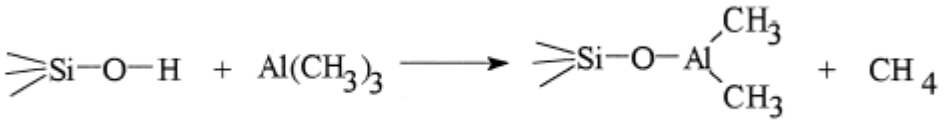

Scheme 2

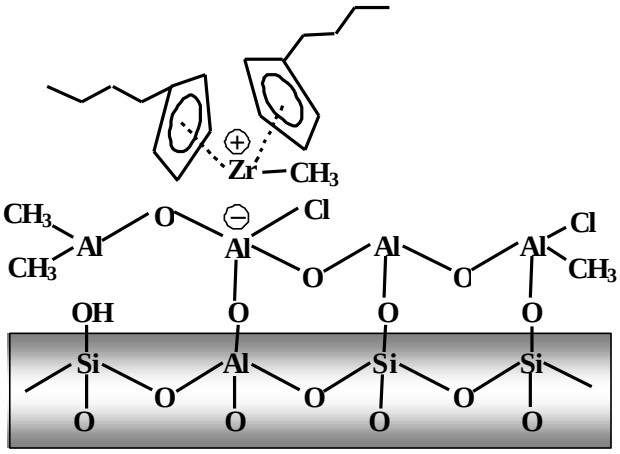

Scheme 3

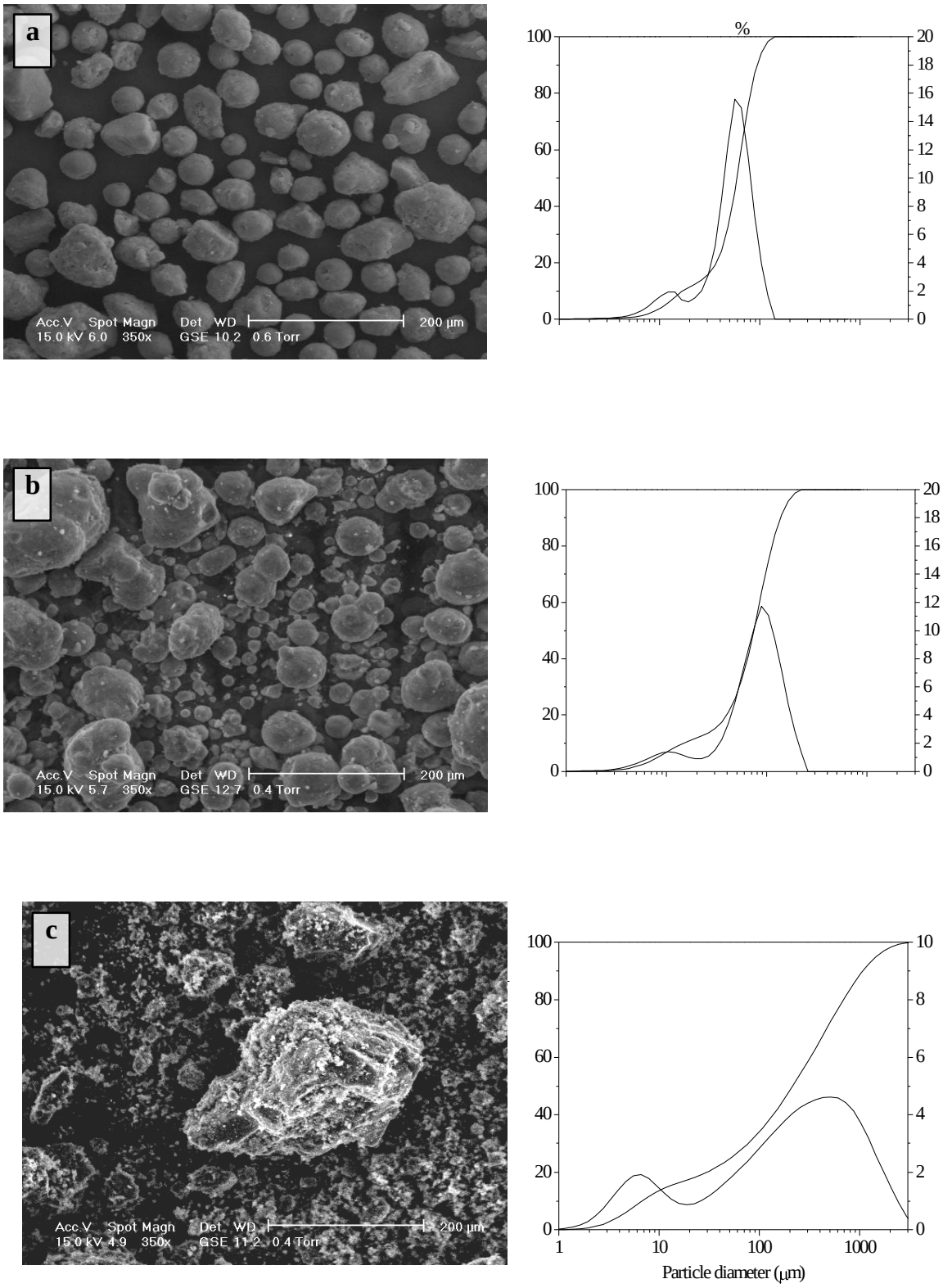
a
Acc.V Spot Magn Det WD 200 µm
15.0 kV 6.0 350x GSE 10.2 0.6 Torr
%
b
Acc.V Spot Magn Det WD 200 µm
15.0 kV 5.7 350x GSE 12.7 0.4 Torr
c
Acc.V Spot Magn Det WD 200 µm
15.0 kV 4.9 350x GSE 11.2 0.4 Torr
Particle diameter (µm)

Figure 1

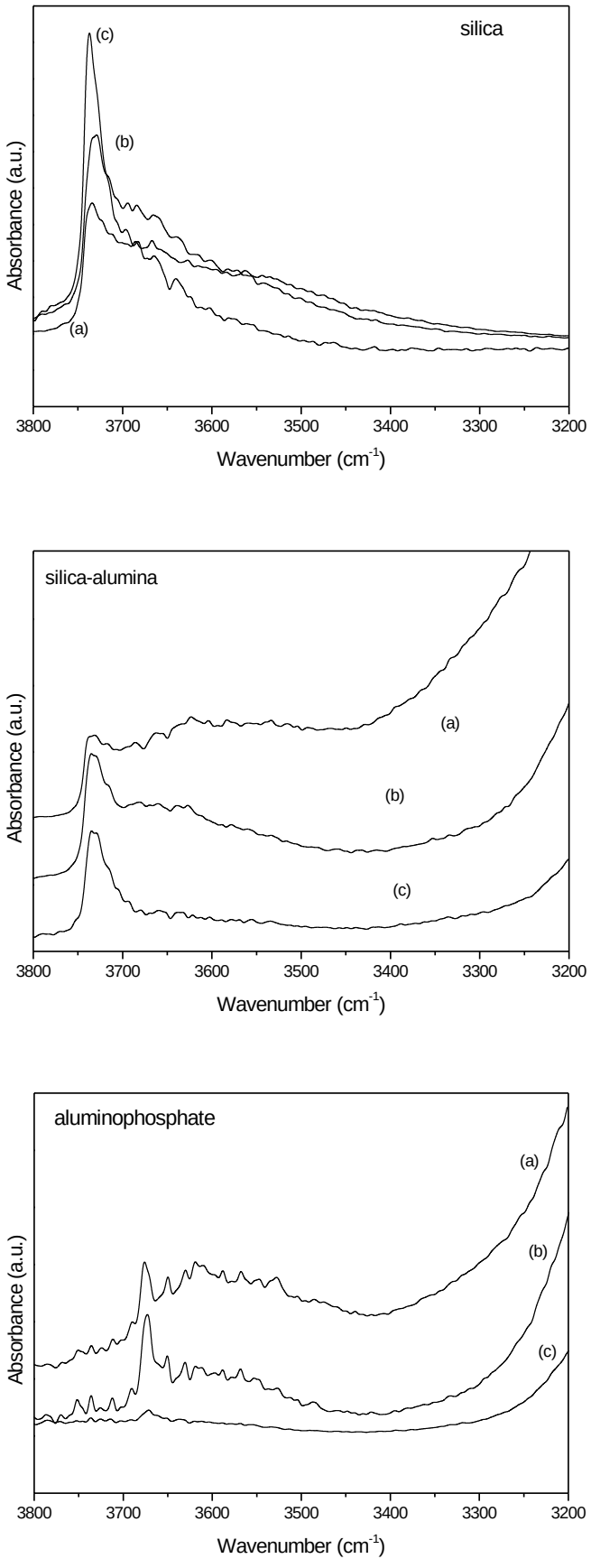
silica
(c)
(b)
(a)
Absorbance (a.u.)
3800
3700
3600
3500
3400
3300
3200
Wavenumber (cm-1)
silica-alumina
(a)
(b)
(c)
Absorbance (a.u.)
3800
3700
3600
3500
3400
3300
3200
Wavenumber (cm-1)
aluminophosphate
(a)
(b)
(c)
Absorbance (a.u.)
3800
3700
3600
3500
3400
3300
3200
Wavenumber (cm-1)

Figure 2.

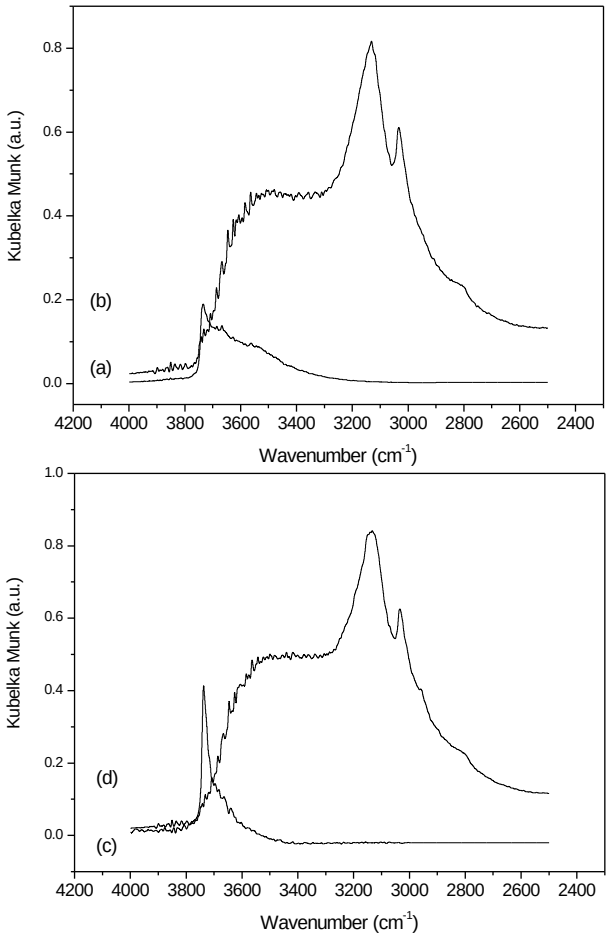
Kubelka Munk (a.u.)
0.0
0.2
0.4
0.6
0.8
(b)
(a)
4200 4000 3800 3600 3400 3200 3000 2800 2600 2400
Wavenumber (cm-1)
Kubelka Munk (a.u.)
0.0
0.2
0.4
0.6
0.8
1.0
(d)
(c)
4200 4000 3800 3600 3400 3200 3000 2800 2600 2400
Wavenumber (cm-1)

Figure 3.

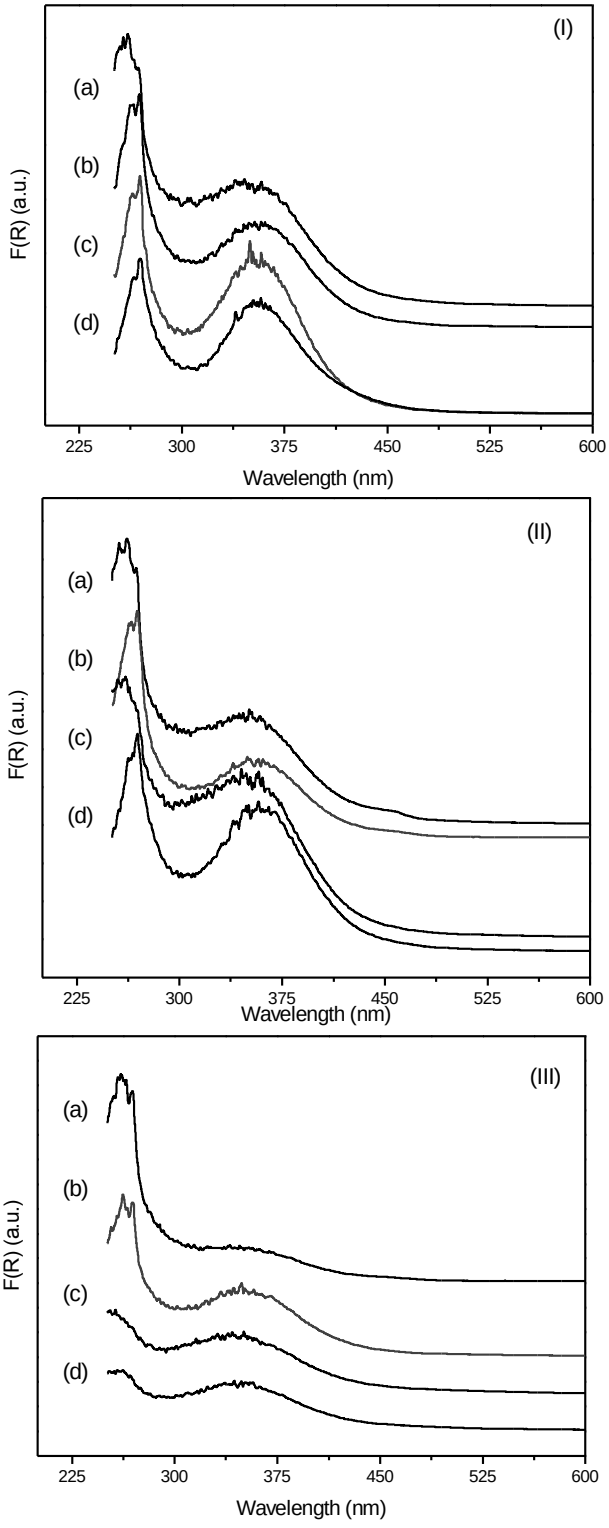
(I)
(a)
(b)
(c)
(d)
F(R) (a.u.)
225
300
375
450
525
600
Wavelength (nm)
(II)
(a)
(b)
(c)
(d)
F(R) (a.u.)
225
300
375
450
525
600
Wavelength (nm)
(III)
(a)
(b)
(c)
(d)
F(R) (a.u.)
225
300
375
450
525
600
Wavelength (nm)

Figure 4.

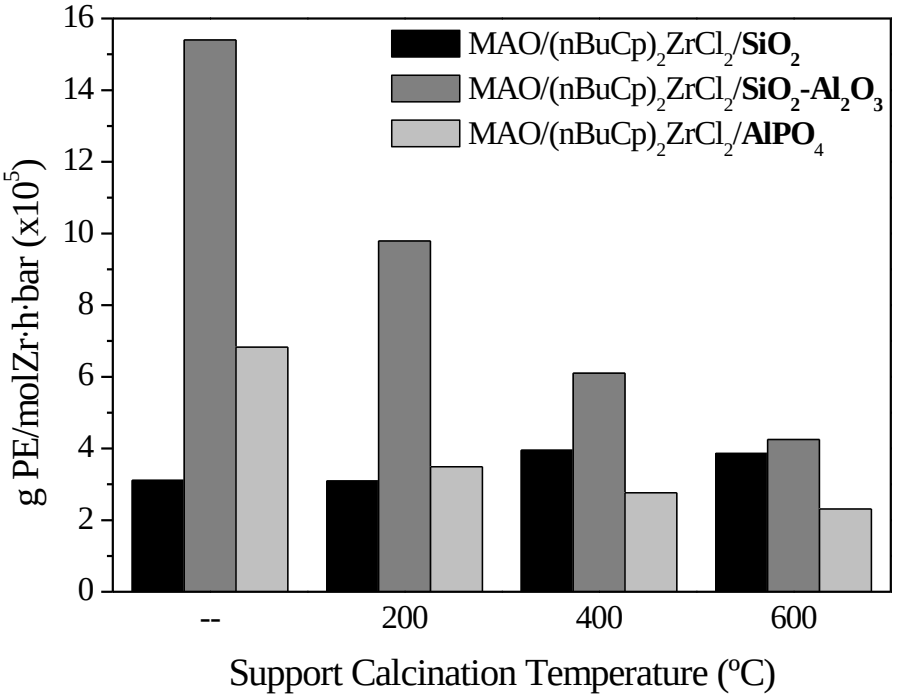
MAO/(nBuCp)2ZrCl2/SiO2
MAO/(nBuCp)2ZrCl2/SiO2-Al2O3
MAO/(nBuCp)2ZrCl2/AlPO4
g PE/molZr·h·bar (x10^5)
0
2
4
6
8
10
12
14
16
--
200
400
600
Support Calcination Temperature (°C)

Figure 5.

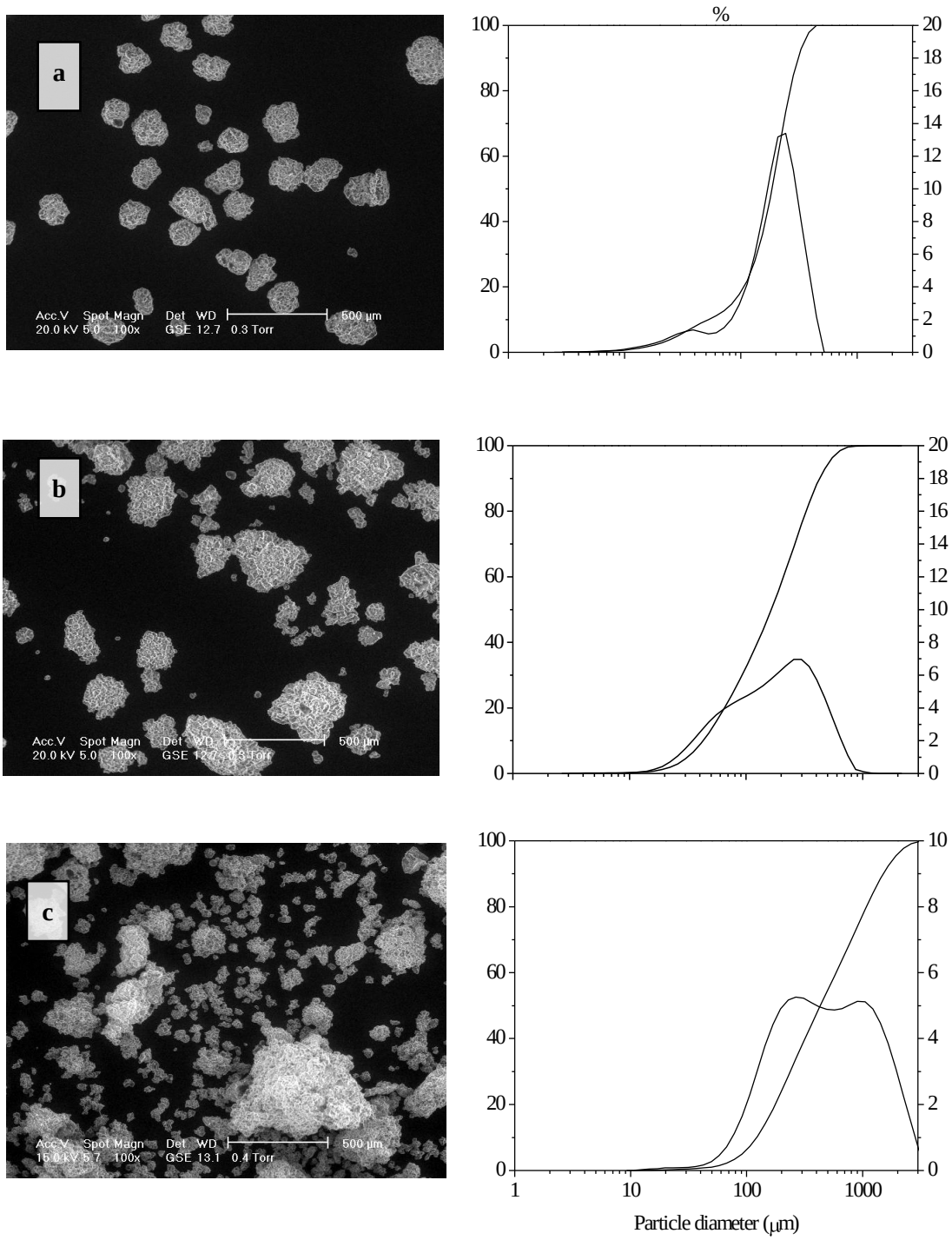
a
Acc.V Spot Magn Det WD 500 µm
20.0 kV 5.0 100x GSE 12.7 0.3 Torr
%
b
c
Particle diameter (µm)

Figure 6.